Robust Control Synthesis Techniques for Multirate and Multisensing Track-Following Servo Systems in Hard Disk Drives

Ryozo Nagamune
Department of Mechanical Engineering,
University of British Columbia,
Vancouver, BC, V6T 1Z4, Canada
e-mail: nagamune@mech.ubc.ca

Xinghui Huang
Seagate Technology,
389 Disc Drive,
Longmont, CO 80503
e-mail: xinghui.huang@seagate.com

Roberto Horowitz
Department of Mechanical Engineering,
University of California,
Berkeley, CA 94720-1740
e-mail: horowitz@berkeley.edu

This paper proposes controller design methods, specially for track-following control of the magnetic read/write head in a hard disk drive (HDD). The servo system to be considered is a general dual-stage multisensing system, which encompasses most of the track-following configurations encountered in the HDD industry, including the traditional single-stage system. For the general system, a robust track-following problem is formulated as a time-varying version of the robust H_2 synthesis problem. Both dynamic and real parametric uncertainties, which are typical model uncertainties in track-following control, are taken into account in the formulation. Three optimal robust controller design techniques with different robustness guarantees are applied to solve the synthesis problem. These are mixed H_2/H_∞, mixed H_2/μ, and robust H_2 syntheses. Advantages and disadvantages of each method are presented. Multirate control, which is inherent to control problems in HDDs, is obtained by reducing multirate problems into linear time-invariant ones, for which there are many useful theories and algorithms available. Most of the techniques proposed in this paper heavily rely on efficient numerical tools for solving linear matrix inequalities. [DOI: 10.1115/1.4000835]

1 Introduction

Track-following control of the magnetic read/write head in hard disk drives (HDDs) is of great importance in meeting recent and future requirements of extremely high track density. For a given system consisting of several components such as a suspension, sensors, and actuators, servo control should achieve optimal track-following performance to meet several objectives. Optimal control will not only realize small track-misregistration but also give us useful information regarding the limitations of a given system, as well as useful information on how to modify the system structure.

In addition to optimality, *robustness* is essential in track-following control. This is because there are many disturbances affecting the control system, such as measurement noise, track runout, windage, and external shock. Moreover, a controller has to be designed so that it maintains acceptable track-following performance for hundreds of thousands of HDD units with slightly different dynamics.

This paper proposes several robust and optimal control methods for a general servo system, called the dual-stage multisensing (DSMS) system. The DSMS system has two actuators and several sensor measurements, and is expected to be necessary for achieving the highly precise track-following that will be required in future HDDs. For this multivariable control system, it is not easy to systematically design a controller that provides both optimality and robustness by using classical control theory. Therefore, we will apply advanced robust control theories such as mixed H_2/H_∞, mixed H_2/μ, and robust H_2 syntheses, to the present multivariable control problem.

In order to enhance performance, we should exploit the freedom of using different sampling/hold rates in the DSMS system. In HDDs, the sampling rate of the position error signal (PES) is determined by the disk spinning speed and the number of servo sectors, while the sampling/hold rates of other sensors, such as a sensor measuring the head relative to the suspension tip, or a vibration sensor in the suspension, are flexible. It is natural to presume that an increase in these rates will improve track-following performance. In this paper, we will assume arbitrary sampling/hold rates.

The paper is organized as follows: In Sec. 2, a multirate robust track-following problem is formulated mathematically. Sec. 3 reviews the method in Refs. [1,2] for the reduction in multirate control problems to time-invariant control ones. Section 4 presents three robust control design methods that solve the formulated robust track-following problem approximately. Section 5 gives a simple example for the synthesis of a dual-stage track-following controller using the robust H_2 synthesis technique. The linear matrix inequalities (LMIs) used in this paper are presented in the Appendixes A and B.

Even though this paper assumes a general structure for a dual-stage multisensing system, it plays a role in theoretically supporting the multirate, multi-input multi-output (MIMO) controller synthesis techniques used in Ref. [3], which presents a comparison of sequential single-input single-output (SISO) and MIMO track-following control synthesis techniques for dual-stage and multisensing servo systems in hard disk drives. Readers are referred to Ref. [3] for more background on the track-following control of dual-stage servo systems for HDDs and for further simulation results of the controller synthesis techniques presented in this paper.

2 A Robust Track-Following Control Problem

In this section, we will formulate a multirate robust track-following control problem to be tackled in this paper. The formulation is general enough to cover most of the track-following control problems encountered in the magnetic disk drive industry,

Contributed by the Dynamic Systems Division of ASME for publication in the JOURNAL OF DYNAMIC SYSTEMS, MEASUREMENT, AND CONTROL. Manuscript received September 28, 2005; final manuscript received June 30, 2009; published online February 2, 2010. Assoc. Editor: Yossi Chait.

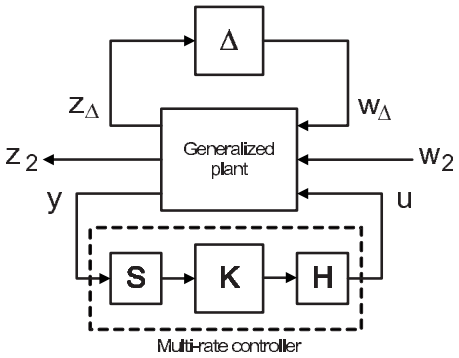

Fig. 1 A generalized plant with an uncertainty block Δ and a multirate controller *HKS*

such as single- and dual-stage controls, irrespective of the type of the secondary actuator, and the locations/number of sensors. Practical examples of track-following control, which reduces to the formulation given below, are presented in Sec. 5, as well as in Ref. [3].

Let us consider a discrete-time[1] linear time-invariant generalized plant with an uncertainty block (see Fig. 1)

$$\begin{bmatrix} z_\Delta \\ z_2 \\ y \end{bmatrix} = \left[\begin{array}{c|ccc} A & B_\Delta & B_2 & B_u \\ \hline C_\Delta & D_{\Delta\Delta} & D_{\Delta 2} & D_{\Delta u} \\ C_2 & D_{2\Delta} & D_{22} & D_{2u} \\ C_y & D_{y\Delta} & D_{y2} & 0 \end{array}\right] \begin{bmatrix} w_\Delta \\ w_2 \\ u \end{bmatrix} \tag{1}$$

$$w_\Delta = \Delta z_\Delta \tag{2}$$

where we have used the standard notation:

$$\left[\begin{array}{c|c} A & B \\ \hline C & D \end{array}\right] := D + C(zI - A)^{-1}B \tag{3}$$

Here, u is the input vector of length 2, which consists of signals to the voice coil motor (VCM) and an auxiliary mini- or microactuator, y is the measurement vector (of any length), typically consisting of the PES, the suspension vibration signal measured by PZT sensors, the position of the magnetic head relative to the gimbal, as measured by a microactuator relative position sensor, and so on, z_2 is the control output vector, typically consisting of the PES and input amplitudes, and w_2 is the disturbance vector of all undesirable signals, such as the track runout, windage, and measurement noise. All the matrices in Eq. (1) are constant and assumed to have compatible dimensions. The generalized plant is comprised of the VCM and secondary actuator dynamics, as well as weighting functions.

The uncertainty block Δ is assumed to be a diagonal matrix in the set

$$\mathcal{B} := \left\{ \begin{array}{c} \Delta := \mathrm{diag}[\delta_1, \ldots, \delta_p, \Delta_V, \Delta_M] \\ \delta_j \in B\mathbb{R}, j = 1, \ldots, p \\ \Delta_V \in BH_\infty, \ \Delta_M \in BH_\infty \end{array} \right\} \tag{4}$$

where p is the number of parametric uncertainties, and

$$B\mathbb{R} := \{r \in \mathbb{R} : |r| \le 1\}$$

$$BH_\infty := \{f \in H_\infty : \|f\|_\infty \le 1\}$$

The real uncertainty δ_j is interpreted as a parameter variation in the dynamics of the VCM and the auxiliary actuator, such as gain, damping ratio, and resonance frequency. Dynamic uncertainties Δ_V and Δ_M are typically due to high-frequency unmodeled dynamics in the VCM and the secondary microactuator, respectively.

Remark 1. It may happen that some parametric uncertainties appear repeatedly as $\delta_j I$. However, since the subsequent discussions are almost unchanged even in such cases, we just consider the case of nonrepeated parametric uncertainties.

Denote the operator from w_2 to z_2 by $T_{z_2 w_2}$. This operator depends on the uncertainty Δ and a multirate controller *HKS*, where S and H mean a multirate sampler and a multirate hold, respectively. Thus, we show the dependence explicitly as $T_{z_2 w_2}(HKS, \Delta)$. Note that the operator $T_{z_2 w_2}(HKS, \Delta)$ is time-varying in general due to the multirate sampler and hold. Then, a multirate robust track-following control problem can be formulated as follows.

PROBLEM 1. *For given multirate sampler S and hold H with fixed sampling and hold rates, design a controller K that stabilizes exponentially the closed-loop system for all* $\Delta \in \mathcal{B}$*, and minimizes the worst-case rms value of* z_2 *against Gaussian white noise* w_2*, or equivalently, solve the optimization problem*

$$\min_{K \in \mathcal{K}(\mathcal{B})} \max_{\Delta \in \mathcal{B}} \|T_{z_2 w_2}(HKS, \Delta)\|_2 \tag{5}$$

where $\mathcal{K}(\mathcal{B})$ *is the set of all controllers that exponentially stabilize the closed-loop system for all* $\Delta \in \mathcal{B}$*, and* $\|\cdot\|_2$ *denotes the* ℓ_2 *semi-norm defined for time-varying systems in p. 73 of Ref. [4].*

This is a multirate robust performance synthesis problem with parametric and dynamic uncertainties. We remark that this problem is general in that it contains, as special cases, single-stage, single-sensing, as well as single-rate cases.

Unfortunately, the formulated problem is difficult to solve exactly with existing control theory and computational tools, because of the nonconvexity and relatively large size of the typical track-following control problem. Therefore, in Sec. 4, we will present design methods to solve this problem in certain approximate cases.

3 Multirate Control

Before proceeding with the exposition of control design techniques for the formulated robust performance synthesis problem, in this section, we will review a way to transform a multirate control problem into a time-invariant one, for which there are many useful theories and numerical algorithms available. To this end, we follow the techniques used in Refs. [2,1,4]. For the ease of notation, only in this section, we remove the uncertainty block Δ, as well as the signals z_Δ and w_Δ, and consider a simplified generalized plant

$$\begin{bmatrix} z_2 \\ y \end{bmatrix} = \left[\begin{array}{c|cc} A & B_2 & B_u \\ \hline C_2 & D_{22} & D_{2u} \\ C_y & D_{y2} & 0 \end{array}\right] \begin{bmatrix} w_2 \\ u \end{bmatrix} \tag{6}$$

However, even with the uncertainty block Δ and corresponding channels w_Δ and z_Δ, the argument in this section remains analogous.

3.1 Reduction in Time-Varying Control. First, by combining the generalized plant with the multirate sampler and hold, we will obtain a periodic time-varying system (see Fig. 2). The explicit form of such a system will be derived next.

A multirate sampler S is expressed mathematically as

$$S: \bar{y}(k) = \Gamma(k) y(k), \quad k = 0, 1, 2, \ldots \tag{7}$$

where $\Gamma(k)$ is a diagonal matrix with diagonal entries of 0 or 1. If the ith measurement is sampled at time k, the (i,i)-entry of $\Gamma(k)$ is set to 1; otherwise, it is set to 0. In the single-rate case, $\Gamma(k) = I$ for any $k = 0, 1, 2, \ldots$. We assume that the sampler is periodic with a period T_s, i.e.

$$\Gamma(k + T_s) = \Gamma(k), \quad k = 0, 1, 2, \ldots \tag{8}$$

[1]Throughout this paper, we assume that, if a plant model is originally given in continuous-time, it has been discretized with the fastest sampling/hold rate.

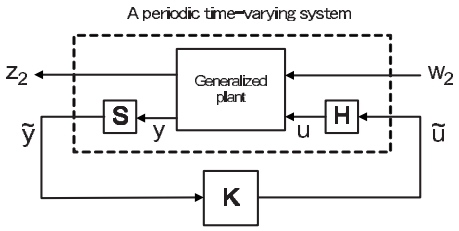

Fig. 2 A periodic time-varying system consisting of a time-invariant generalized plant, a multirate sampler *S*, and a multirate hold *H*

To represent a multirate hold H mathematically, we decompose the input vector u into vectors with the fastest and slower hold rates, as follows:

$$u =: \begin{bmatrix} u_s \\ u_f \end{bmatrix} \tag{9}$$

where the subscripts s and f stand for *slower* and *fastest* respectively, and channels with slower sampling rates are gathered at the top of the vector u without loss of generality. Here, the term "fastest rate" refers to the fastest rate among not only hold rates, but also sampling rates. Thus, if the fastest sampling rate is faster than any hold rate u consists of only u_s. Then, the hold is a mapping

$$H:\tilde{u} := \begin{bmatrix} \tilde{u}_s \\ \tilde{u}_f \end{bmatrix} \to \begin{bmatrix} u_s \\ u_f \end{bmatrix} \tag{10}$$

which can be described as a dynamic linear time-varying system

$$\begin{bmatrix} x_h(k+1) \\ \begin{bmatrix} u_s(k) \\ u_f(k) \end{bmatrix} \end{bmatrix} = \begin{bmatrix} A_h(k) & B_h(k) \\ C_h(k) & D_h(k) \end{bmatrix} \begin{bmatrix} x_h(k) \\ \begin{bmatrix} \tilde{u}_s(k) \\ \tilde{u}_f(k) \end{bmatrix} \end{bmatrix} \tag{11}$$

where x_h is the state vector of H, and for $k=0,1,2,\ldots$

$$A_h(k) := I_{n_s} - \Omega(k), \quad B_h(k) := [\Omega(k), 0]$$

$$C_h(k) := \begin{bmatrix} I_{n_s} - \Omega(k) \\ 0 \end{bmatrix}, \quad D_h(k) := \begin{bmatrix} \Omega(k) & 0 \\ 0 & I_{n_f} \end{bmatrix} \tag{12}$$

Here, the dimensions of u_s and u_f are denoted by n_s and n_f, respectively, $\Omega(k) \in \mathbb{R}^{n_s \times n_s}$ is a diagonal matrix with diagonal entries of 0 or 1, and plays a similar role to $\Gamma(k)$ in Eq. (8). If we feed the ith input signal of $\tilde{u}_s$ from the controller at time k, then (i,i)-entry of $\Omega(k)$ is set to 1; otherwise, it is set to 0, resulting in the ith input at time k equal to the ith input at time $k-1$. In the single-rate case, the hold degenerates to a static system $u(k) = \tilde{u}(k)$. We assume that the hold is periodic with a period T_h, i.e.

$$\Omega(k + T_h) = \Omega(k), \quad k = 0,1,2,\ldots \tag{13}$$

Now, we suppose that the periods T_s and T_h are rationally related, that is, their least common multiple

$$T := \mathrm{lcm}(T_s, T_h) \tag{14}$$

is an integer. Then, by combining Eqs. (6), (7), and (11), we obtain a linear periodic time-varying system with the period T

$$\begin{bmatrix} \tilde{x}(k+1) \\ z_2(k) \\ \tilde{y}(k) \end{bmatrix} = \begin{bmatrix} \tilde{A}(k) & \tilde{B}_2(k) & \tilde{B}_u(k) \\ \tilde{C}_2(k) & \tilde{D}_{22}(k) & \tilde{D}_{2u}(k) \\ \tilde{C}_y(k) & \tilde{D}_{y2}(k) & 0 \end{bmatrix} \begin{bmatrix} \tilde{x}(k) \\ w_2(k) \\ \tilde{u}(k) \end{bmatrix} \tag{15}$$

for $k=0,1,2,\ldots$, where the matrices in Eq. (15) are obtained by straightforward calculation, as follows:

$$\tilde{A}(k) := \begin{bmatrix} A & B_u C_h(k) \\ 0 & A_h(k) \end{bmatrix}$$

$$\tilde{B}_2(k) := \begin{bmatrix} B_2 \\ 0 \end{bmatrix}, \quad \tilde{B}_u(k) := \begin{bmatrix} B_u D_h(k) \\ B_h(k) \end{bmatrix}$$

$$\tilde{C}_2(k) := \begin{bmatrix} C_2 & D_{2u} C_h(k) \end{bmatrix}$$

$$\tilde{C}_y(k) := \Gamma(k) \begin{bmatrix} C_y & 0 \end{bmatrix}$$

$$\tilde{D}_{22}(k) := D_{22}, \quad \tilde{D}_{2u}(k) := D_{2u} D_h(k)$$

$$\tilde{D}_{y2}(k) := \Gamma(k) D_{y2} \tag{16}$$

Note that system (15) includes all the information about the multirate sampler and hold.

3.2 Reduction in Time-Invariant Control. Next, we will apply known controller design methods for time-varying systems to system (15), thereby obtaining a multirate controller.

It is proven in Refs. [4,1,2] that many important control synthesis problems for time-varying systems can be solved in a very similar way to those for time-invariant systems. Moreover, for *periodic* time-varying systems, these problems can be reduced to finite-dimensional convex optimization problems, which can be solved by using efficient numerical techniques for LMIs.

To be more concrete, using the matrices in the periodic time-varying plant (Eq. (15)) with its period T, let us consider an auxiliary linear time-invariant system

$$\left[\begin{array}{c} \boldsymbol{z}_2 \\ \boldsymbol{y} \end{array}\right] = \left[\begin{array}{c|cc} \boldsymbol{ZA} & \boldsymbol{ZB}_2 & \boldsymbol{ZB}_u \\ \hline \boldsymbol{C}_2 & \boldsymbol{D}_{22} & \boldsymbol{D}_{2u} \\ \boldsymbol{C}_y & \boldsymbol{D}_{y2} & 0 \end{array}\right] \left[\begin{array}{c} \boldsymbol{w}_2 \\ \boldsymbol{u} \end{array}\right] \tag{17}$$

Here, matrices with bold capital letters are block-diagonal,[2] consisting of the matrices in (Eq. (15)); for example

$$\boldsymbol{A} := \begin{bmatrix} \tilde{A}(0) & & \\ & \ddots & \\ & & \tilde{A}(T-1) \end{bmatrix} \tag{18}$$

and Z is a "shift" matrix, which is of compatible size with $\boldsymbol{A}$ and defined by

$$Z := \begin{bmatrix} 0 & \cdots & 0 & I \\ I & & & 0 \\ & \ddots & & \vdots \\ & & I & 0 \end{bmatrix} \tag{19}$$

The vectors $\boldsymbol{z}_2$, $\boldsymbol{w}_2$, $\boldsymbol{y}$, and $\boldsymbol{u}$ are considered as "lifted" signals of z_2, w_2, $\tilde{y}$, and $\tilde{u}$ in (Eq. (15)), respectively.

By a combination of the theories in Refs. [4,1,2], we can deduce the following equivalences:

- A time-invariant controller

[2]Throughout this paper, we use bold capital letters to denote block-diagonal matrices.

$$\boldsymbol{u} = \left[\begin{array}{c|c} \boldsymbol{ZK}_A & \boldsymbol{ZK}_B \\ \hline \boldsymbol{K}_C & \boldsymbol{K}_D \end{array}\right] \boldsymbol{y} \tag{20}$$

stabilizes the time-invariant system (17), and satisfies a H_2 or H_∞ norm condition

$$\|T_{z_2 w_2}\|_i < \begin{cases} \sqrt{T\gamma^2}, & \text{if } i = 2 \\ \gamma, & \text{if } i = \infty \end{cases} \tag{21}$$

where T is defined in Eq. (14). Here, the matrices in Eq. (20) are block-diagonal, and we denote them as

$$\boldsymbol{K}_M := \begin{bmatrix} K_M(0) & & \\ & \ddots & \\ & & K_M(T-1) \end{bmatrix} \tag{22}$$

where M can be A, B, C, or D, and the block sizes in Z are compatible with the block sizes in $\boldsymbol{K}_A$.

- A periodic time-varying controller

$$\begin{bmatrix} x_K(k+1) \\ \tilde{u}(k) \end{bmatrix} = \begin{bmatrix} K_A(k) & K_B(k) \\ K_C(k) & K_D(k) \end{bmatrix} \begin{bmatrix} x_K(k) \\ \tilde{y}(k) \end{bmatrix} \tag{23}$$

of the period T stabilizes exponentially the time-varying system (15), and satisfies a norm condition

$$\|T_{z_2 w_2}\|_i < \gamma, \quad i = 2 \text{ or } \ell_2\text{-induced} \tag{24}$$

In this way, the ℓ_2 seminorm or ℓ_2-induced norm suboptimal control problem for a periodic time-varying system can be transformed into a standard H_2 or H_∞ suboptimal control problem for a time-invariant system, with a controller structure (Eqs. (20) and (22)). The controller structure can be guaranteed by solving the suboptimal control problems with numerical tools for LMIs.

To summarize, our procedure to solve the multirate control problem is

1. Derive a time-invariant system (17).
2. Design a controller (20) for Eq. (17).
3. Obtain a periodic time-varying controller (23) by decomposing controller matrices as Eq. (22).

4 Robust Controller Design

In this section, we will present three robust controller design methods useful for robust track-following: mixed H_2/H_∞, mixed H_2/μ, and robust H_2 syntheses. These methods are based on convex optimization involving LMIs, to which there are numerically efficient algorithms [5] and software [6–8] available. Some of the LMIs, which are necessary to solve the optimization problems, will be given in the Appendixes A and B. Advantages and disadvantages of each method will be summarized.

4.1 Mixed H_2/H_∞ Synthesis. The mixed H_2/H_∞ synthesis is a well-known design method for reconciling performance and robustness [9,10]. Since this approach can deal with only unstructured dynamic uncertainties, we will ignore parametric uncertainties in Δ. In this approach, we can guarantee only robust stability for individual, not simultaneous, perturbations of Δ_V and Δ_M (see Fig. 3).

Denote the set of all controllers that stabilize the closed-loop system in Fig. 3 for $\Delta_V \in BH_\infty$ and for $\Delta_M \in BH_\infty$ by $\mathcal{K}_V$ and $\mathcal{K}_M$, respectively. Then, the control problem in this approach is formally stated: as follows:

PROBLEM 2. *For given multirate sampler S and hold H with fixed sampling and hold rates, design a controller K that exponentially stabilizes the closed-loop system for all $\Delta_V \in BH_\infty$ and $\Delta_M \in BH_\infty$, and minimizes the nominal rms value of z_2 against Gaussian white noise w_2, or equivalently, solve the optimization problem*

$$\min_{K \in \mathcal{K}_V \cap \mathcal{K}_M} \|T_{z_2 w_2}(HKS,0)\|_2 \tag{25}$$

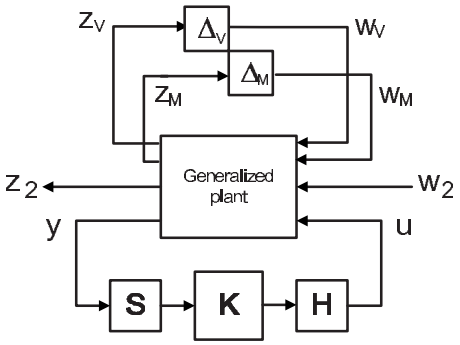

Fig. 3 Uncertainty structure for mixed H_2/H_∞ synthesis

This problem can be rewritten, as follows:

$$\min_K \gamma, \text{ subject to} \begin{cases} \|T_{z_2 w_2}(HKS,0)\|_2 < \gamma \\ \|T_{z_V w_V}(HKS)\|_{\ell_2} < 1 \\ \|T_{z_M w_M}(HKS)\|_{\ell_2} < 1 \end{cases} \tag{26}$$

where z_V, z_M, w_V, and w_M are signals shown in Fig. 3, and $\|\cdot\|_{\ell_2}$ means the ℓ_2-induced norm. We can solve the optimization (26) by following the procedure given at the end of Sec. 3. An auxiliary time-invariant system corresponding to Eq. (17) can be expressed in this case as

$$G: \begin{bmatrix} \boldsymbol{w}_V \\ \boldsymbol{w}_M \\ \boldsymbol{w}_2 \\ \boldsymbol{u} \end{bmatrix} \to \begin{bmatrix} \boldsymbol{z}_V \\ \boldsymbol{z}_M \\ \boldsymbol{z}_2 \\ \boldsymbol{y} \end{bmatrix}$$

$$G(z) := \left[\begin{array}{c|cccc} \boldsymbol{ZA} & \boldsymbol{ZB}_V & \boldsymbol{ZB}_M & \boldsymbol{ZB}_2 & \boldsymbol{ZB}_u \\ \hline \boldsymbol{C}_V & \boldsymbol{D}_{VV} & \boldsymbol{D}_{VM} & \boldsymbol{D}_{V2} & \boldsymbol{D}_{Vu} \\ \boldsymbol{C}_M & \boldsymbol{D}_{MV} & \boldsymbol{D}_{MM} & \boldsymbol{D}_{M2} & \boldsymbol{D}_{Mu} \\ \boldsymbol{C}_2 & \boldsymbol{D}_{2V} & \boldsymbol{D}_{2M} & \boldsymbol{D}_{22} & \boldsymbol{D}_{2u} \\ \boldsymbol{C}_y & \boldsymbol{D}_{yV} & \boldsymbol{D}_{yM} & \boldsymbol{D}_{y2} & 0 \end{array}\right] \tag{27}$$

where all the block matrices are obtained by the transformation process from multirate control to time-invariant control presented in Sec. 3. Using the system matrices, the inequality conditions in Eq. (26) can be expressed as LMI conditions [11,12], which are given in Appendix B.1.

Main advantages of the mixed H_2/H_∞ method in track-following control are that the computational cost involved in finding a solution to Eq. (26) is relatively low, and that an optimal solution is guaranteed to be obtained given a feasible condition. While the robust H_2 synthesis methodology, which will be presented later, involves the iterative solution of convex optimization problems in order to solve for a nonconvex one, the mixed H_2/H_∞ method requires the solution of just one convex problem. However, a disadvantage of this method is that it can neither deal with structured uncertainties, nor guarantee robust performance. In other words, there is no guarantee that robustness in our original problem (Problem 1) is indeed satisfied by the mixed H_2/H_∞ design.

4.2 Mixed H_2/μ Synthesis. The μ-theory is a powerful tool to deal with various types of uncertainties in robust control [13]. If the performance is evaluated with the ℓ_2-induced (or H_∞) norm, one can design a controller for robust performance via the so-called *D-K* iterations in the μ-synthesis theory. However, since the performance measure in the present problem is the ℓ_2 seminorm (or H_2 norm), we cannot use the μ-synthesis theory as it is. Here, we combine the *D-K* iteration with the mixed H_2/H_∞ syn-

thesis to design a controller to achieve nominal performance optimization with guaranteed robust stability. To be more precise, we consider the following problem:

PROBLEM 3. *For given multirate sampler S and hold H with fixed sampling and hold rates, design a controller K that stabilizes the closed-loop system for all* $\Delta \in \mathcal{B}$*, and minimizes the nominal rms value of* z_2 *against Gaussian white noise* w_2*, i.e., solve the optimization problem*

$$\min_{K \in \mathcal{K}(\mathcal{B})} \|T_{z_2 w_2}(HKS,0)\|_2 \tag{28}$$

Notice that the only difference between Eqs. (28) and (5) is that the term $\max_{\Delta \in \mathcal{B}}$ is not taken into consideration in Eq. (28), and thus we optimize only nominal performance.

Let us first consider a simpler situation, where $\tilde{K}$ is a single-rate controller. Then, by μ-analysis theory [13,14], the condition $\tilde{K} \in \mathcal{K}(\mathcal{B})$ can be guaranteed by $\tilde{K} \in \mathcal{K}(0)$ (nominally stabilizing) and

$$\|DT_{z_\Delta w_\Delta}(\tilde{K})D^{-1}\|_\infty < 1 \tag{29}$$

for some matrix function $D \in \mathcal{D}$. Here, $\mathcal{D}$ is a set of matrix functions associated with $\mathcal{B}$ in Eq. (4) and defined by

$$\mathcal{D} := \left\{ \begin{matrix} D := \mathrm{diag}[d_1, \ldots, d_{p+2}] \\ d_j \in H_\infty, d_j^{-1} \in H_\infty, j = 1, \ldots, p+2 \end{matrix} \right\} \tag{30}$$

Therefore, problem (28) can be solved via mixed H_2/H_∞ optimization with D-scaling

$$\min_{\tilde{K} \in \mathcal{K}(0), D \in \mathcal{D}} \gamma, \text{ subject to} \begin{cases} \|T_{z_2 w_2}(\tilde{K},0)\|_2 < \gamma \\ \|DT_{z_\Delta w_\Delta}(\tilde{K})D^{-1}\|_\infty < 1 \end{cases} \tag{31}$$

Using the single-rate result, it is possible to solve the above multirate control problem approximately, with the following procedures:

1. Design a rational matrix $D \in \mathcal{D}$, as well as a single-rate controller $\tilde{K}$ with the fastest sampling/hold rate (or a continuous-time controller if a generalized plant is given in continuous-time), that solves the optimization

$$\inf_{D \in \mathcal{D}, \tilde{K} \in \mathcal{K}(0)} \|DT_{z_\Delta w_\Delta}(\tilde{K})D^{-1}\|_\infty \tag{32}$$

2. Using the D obtained in Step 1, solve a multirate mixed H_2/H_∞ problem

$$\min_{K \in \mathcal{K}(0)} \gamma, \text{ sub. to} \begin{cases} \|T_{z_2 w_2}(HKS,0)\|_2 < \gamma \\ \|DT_{z_\Delta w_\Delta}(HKS)D^{-1}\|_{\ell_2} < 1 \end{cases} \tag{33}$$

We remark that the constraint

$$\|DT_{z_\Delta w_\Delta}(HKS)D^{-1}\|_{\ell_2} < 1 \tag{34}$$

guarantees closed-loop stability for all $\Delta \in \mathcal{B}$, due to the Small Gain Theorem. The optimization problem (32) in step 1 can be solved via *D-K* iteration with "μ-Analysis and Synthesis Toolbox" (or the latest "Robust Control Toolbox") in MATLAB [15]. On the other hand, since the optimization problem (33) is of the same type as (26), the technique outlined in Sec. 4.1 can be used to solve the optimization in step 2.

The main advantage of the proposed mixed H_2/μ synthesis, as compared with the mixed H_2/H_∞ synthesis, is the freedom in the selection of D. Notice that $D=I$ corresponds to the mixed H_2/H_∞ design. Because of this freedom, we can expect better nominal performance and robust stability. However, one disadvantage is that the problem becomes nonconvex, and therefore, the obtained solution may not be a global optimum. Moreover, the solution may be computationally expensive to obtain, especially when we select a D of high order. In addition, like the mixed H_2/H_∞ approach, there is no guarantee regarding robust performance.

Remark 2. Since our uncertainty set $\mathcal{B}$ includes parametric uncertainties, we can have a less conservative robust stability condition than Eq. (29) (see Refs. [14,16,17]). If we use the less conservative condition, an extra "*G*-scaling" must be introduced. This will increase the computational effort, as well as the final controller order.

Remark 3. It has been our experience that the mixed H_2/μ controller performs better if the performance channel is included in solution to step 1, even though the measure in μ-synthesis is not the H_2 norm but rather the H_∞ norm.

4.3 Robust H_2 Synthesis. The previous two methods cannot handle robust performance, and therefore, plant perturbations may degrade the track-following performance to an unacceptable extent. The third method, which is based on the result in Ref. [18], can guarantee robust performance for parametric uncertainties, but not for dynamic ones.

Define a set $\mathcal{B}_p$ of parametric uncertainties as

$$\mathcal{B}_p := \{\Delta := \mathrm{diag}[\delta_1, \ldots, \delta_p],\ \ \delta_j \in B\mathbb{R},\ \ j = 1, \ldots, p\}. \tag{35}$$

The design problem in this section is stated next.

PROBLEM 4. *For given multirate sampler S and hold H with fixed sampling and hold rates, design a controller K that stabilizes the closed-loop system for all* $\Delta \in \mathcal{B}_p$*, and minimizes the worst-case rms value of* z_2 *against Gaussian white noise* w_2 *for all* $\Delta \in \mathcal{B}_p$*, i.e., solve*

$$\min_{K \in \mathcal{K}(\mathcal{B}_p)} \max_{\Delta \in \mathcal{B}_p} \|T_{z_2 w_2}(HKS,\Delta)\|_2 \tag{36}$$

To use the result in Ref. [18], we need that the following assumptions are satisfied.

ASSUMPTION 1. $D_{\Delta\Delta}=0$ *and* $D_{y\Delta}=0$ in *Eq. (1)*.

The assumption $D_{\Delta\Delta}=0$ guarantees that the closed-loop system matrices depend on Δ affinely (see Eq. (38)), while $D_{y\Delta}=0$ ensures the well-posedness of the closed-loop system by forcing the direct term from u to y to be zero (see Eq. (37)). These assumptions are not restrictive, since they hold most of the track-following problems in HDDs.

In the case with only parametric uncertainties, the uncertain system from $[w_2^T, u^T]^T$ to $[z_2^T, y^T]^T$ is obtained as

$$\left[\begin{matrix} z_2 \\ y \end{matrix}\right] = \left[\begin{array}{c|cc} A^\Delta & B_2^\Delta & B_u^\Delta \\ \hline C_2^\Delta & D_{22}^\Delta & D_{2u}^\Delta \\ C_y & D_{y2} & 0 \end{array}\right] \left[\begin{matrix} w_2 \\ u \end{matrix}\right] \tag{37}$$

where the superscript Δ means a "matrix with uncertainties," and the system matrices are given by

$$\left[\begin{matrix} A^\Delta & B_2^\Delta & B_u^\Delta \\ C_2^\Delta & D_{22}^\Delta & D_{2u}^\Delta \end{matrix}\right] := \left[\begin{matrix} A & B_2 & B_u \\ C_2 & D_{22} & D_{2u} \end{matrix}\right] + \left[\begin{matrix} B_\Delta \\ D_{2\Delta} \end{matrix}\right] \Delta \left[\begin{matrix} C_\Delta & D_{\Delta 2} & D_{\Delta u} \end{matrix}\right] \tag{38}$$

In the robust H_2 method that will be explained below, it is important that the system matrices in Eq. (38) are affine in Δ, and that Δ belongs to a convex polyhedron $\mathcal{B}_p$ (which is a hypercube in the present setting).

To deal with the multirate characteristics of the controller, we use the procedure in Sec. 3. Then, for an augmented time-invariant plant

$$\left[\begin{matrix} z_2 \\ \boldsymbol{y} \end{matrix}\right] = \left[\begin{array}{c|cc} Z\boldsymbol{A}^\Delta & Z\boldsymbol{B}_2^\Delta & Z\boldsymbol{B}_u^\Delta \\ \hline \boldsymbol{C}_2^\Delta & \boldsymbol{D}_{22}^\Delta & \boldsymbol{D}_{2u}^\Delta \\ \boldsymbol{C}_y & \boldsymbol{D}_{y2} & 0 \end{array}\right] \left[\begin{matrix} \boldsymbol{w}_2 \\ \boldsymbol{u} \end{matrix}\right] \tag{39}$$

we need to design a linear time-invariant controller of the form

$$\boldsymbol{u} = \left[\begin{array}{c|c} \boldsymbol{ZK}_A & \boldsymbol{ZK}_B \\ \hline \boldsymbol{K}_C & \boldsymbol{K}_D \end{array}\right]\boldsymbol{y} \tag{40}$$

We remark that all the uncertain matrices in Eq. (39) are affine in Δ. The time-invariant closed-loop system of Eqs. (39) and (40) is expressed as

$$(T_{\mathrm{cl}}(\Theta,\Delta))(z) := \left[\begin{array}{c|c} A_{\mathrm{cl}}(\Theta,\Delta) & B_{\mathrm{cl}}(\Theta,\Delta) \\ \hline C_{\mathrm{cl}}(\Theta,\Delta) & D_{\mathrm{cl}}(\Theta,\Delta) \end{array}\right]$$

$$:= \left[\begin{array}{c|c} \boldsymbol{Z}(A_0^\Delta + \mathfrak{B}^\Delta\Theta\mathfrak{C}) & \boldsymbol{Z}(B_0^\Delta + \mathfrak{B}^\Delta\Theta\mathfrak{D}_{21}) \\ \hline C_0^\Delta + \mathfrak{D}_{12}^\Delta\Theta\mathfrak{C} & D_{22}^\Delta + \mathfrak{D}_{12}^\Delta\Theta\mathfrak{D}_{21} \end{array}\right]$$

where the matrices are defined by

$$\boldsymbol{Z} := \begin{bmatrix} Z & 0 \\ 0 & Z \end{bmatrix}, \quad \Theta := \begin{bmatrix} \boldsymbol{K}_A & \boldsymbol{K}_B \\ \boldsymbol{K}_C & \boldsymbol{K}_D \end{bmatrix}$$

$$A_0^\Delta := \begin{bmatrix} \boldsymbol{A}^\Delta & 0 \\ 0 & 0 \end{bmatrix}$$

$$\mathfrak{B}^\Delta := \begin{bmatrix} 0 & \boldsymbol{B}_u^\Delta \\ I & 0 \end{bmatrix}, \quad B_0^\Delta := \begin{bmatrix} \boldsymbol{B}_2^\Delta \\ 0 \end{bmatrix}$$

$$\mathfrak{C} := \begin{bmatrix} 0 & I \\ \boldsymbol{C}_y & 0 \end{bmatrix}, \quad \mathfrak{D}_{21} := \begin{bmatrix} 0 \\ \boldsymbol{D}_{y2} \end{bmatrix}$$

$$C_0^\Delta := \begin{bmatrix} \boldsymbol{C}_2^\Delta & 0 \end{bmatrix}, \ \mathfrak{D}_{12}^\Delta := \begin{bmatrix} 0 & \boldsymbol{D}_{2u}^\Delta \end{bmatrix}$$

Our problem is to find a robustly stabilizing controller matrix Θ that solves

$$\min_{\Theta} \max_{\Delta\in\mathcal{B}_p} \|T_{\mathrm{cl}}(\Theta,\Delta)\|_2$$

This can be solved by the following optimization, which involves a finite number of matrix inequalities:

$$\min_{\boldsymbol{W},\boldsymbol{P},\Theta} \gamma, \text{ subject to} \begin{cases} \gamma > \mathrm{trace}\boldsymbol{W} \\ \begin{bmatrix} \boldsymbol{W} & C_{\mathrm{cl}}(\Theta,\Delta_k) & D_{\mathrm{cl}}(\Theta,\Delta_k) \\ * & \boldsymbol{P} & 0 \\ * & * & I \end{bmatrix} > 0 \\ \begin{bmatrix} \boldsymbol{P}_Z & \boldsymbol{P}_Z A_{\mathrm{cl}}(\Theta,\Delta_k) & \boldsymbol{P}_Z B_{\mathrm{cl}}(\Theta,\Delta_k) \\ * & \boldsymbol{P} & 0 \\ * & * & I \end{bmatrix} > 0 \end{cases} \tag{41}$$

for $\Delta_k \in \mathcal{V}(\mathcal{B}_p)$. Here, the matrices $\boldsymbol{P}$ and $\boldsymbol{W}$ are block-diagonals of appropriate sizes, $\boldsymbol{P}_Z := \boldsymbol{Z}^T\boldsymbol{P}\boldsymbol{Z}$, $\mathcal{V}(\mathcal{B}_p)$ is the set of all vertices of a convex polyhedron $\mathcal{B}_p$, and the "*-blocks" are the block matrices that make the total matrix symmetric. The replacement of infinitely many inequality constraints for $\Delta \in \mathcal{B}_p$ with finitely many ones at vertices $\Delta_k \in \mathcal{B}_p$ is possible due to the facts that the closed-loop system matrices are affine in Δ, and that the set $\mathcal{B}_p$ is a convex polyhedron.

Unfortunately, this problem is nonconvex, since there are coupling terms between $\boldsymbol{P}$ and Θ in Eq. (41). However, by using the coordinate descent method (see Refs. [19,20] and references therein), we can find a local optimum. The procedure is presented next.

[Initial design of Θ] This will be explained below, as well as in Appendix B.2. Set the result of the initial design to Θ_1. Also, set $i=1$.

[Design of $\boldsymbol{P}$] Fix $\Theta := \Theta_i$. Solve the convex optimization problem (41) with respect to γ, $\boldsymbol{W}$, and $\boldsymbol{P}$. Set a solution $\boldsymbol{P}$ to $\boldsymbol{P}_i$.

[Design of Θ] Fix $\boldsymbol{P} := \boldsymbol{P}_i$. Solve the convex optimization problem (41) with respect to γ, $\boldsymbol{W}$, and Θ. Set a solution Θ to Θ_{i+1}. Increment i by one. Continue this iteration until convergence.

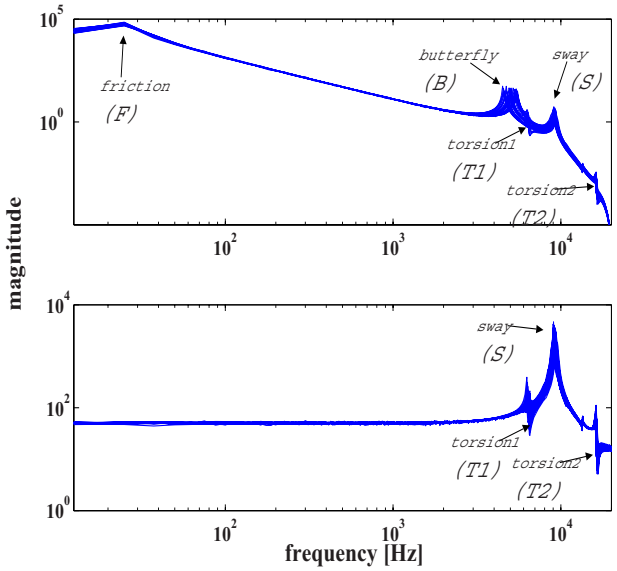

Fig. 4 Frequency responses from u_V to y_{LDV} (upper figure) and from u_M to y_{LDV} (lower figure)

Remark 4. Theoretically, since the value γ is monotonically nonincreasing during the iterations and it has a lower bound (which is 0), it will converge to some positive number. Numerically, we stop the iteration when the value of γ stops decreasing (within some tolerance).

Generally speaking, in nonconvex optimization problems, the selection of an initial point is critical. We follow the procedure given in Ref. [18] to derive a reasonable initial point, which will be reviewed in Appendix B.2.

The advantage of the robust H_2 synthesis over the other synthesis methodologies discussed in this paper is the ability to cope with robust performance in the design. However, to utilize the proposed synthesis technique, it is necessary to ignore dynamic uncertainties, which generally capture high-frequency unmodeled dynamics, typically unavoidable in modeling. In addition, the computation of a solution to the robust H_2 problem is demanding, because we have to solve for a series of convex optimization problems iteratively in order to solve the nonconvex problem. Further, the number of inequality constraints increases exponentially with the number of parametric uncertainties, since the constraints are imposed at vertices of a hypercube $\mathcal{B}_p$. Therefore, only a few parametric uncertainties can be included in a practical design.

5 A Design Example

In this section, we will demonstrate the usefulness of the robust H_2 synthesis method presented in Sec. 4.3 through one simple example of a dual-stage track-following control problem. This example is taken from Ref. [21]. Other examples are shown in Ref. [3]. The system to be considered is a PZT-actuated dual-stage servo system, whose inputs are the VCM input (u_V) and the input to the PZT-actuators (u_M), and whose output is the head position (y_{LDV}) measured by laser Doppler vibrometer (LDV). Readers are referred to Refs. [21–23] and their references for details on the identification, modeling, and control of the PZT-actuated dual-stage servo system discussed in this section.

5.1 Continuous-Time Modeling. In order to use the robust H_2 synthesis technique, we need a mathematical model with only parametric uncertainties. To derive such a mathematical model, 36 frequency responses of P_{VCM} (from u_V to y_{LDV}) and of P_{MA} (from u_M to y_{LDV}) have been taken in Ref. [21], as shown in Fig. 4.

To reduce the computational burden during the controller syn-

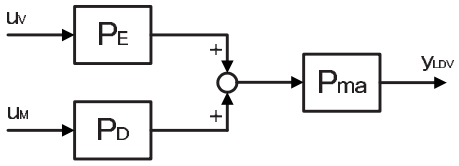

Fig. 5 Block diagram

thesis, it is advantageous to build a model with its order and the number of uncertain parameters as small as possible. As shown in Fig. 4, since the suspension's sway mode (S) and torsion modes ($T1$ and $T2$) can be seen in both frequency responses, these suspension modes can be factored out as a common transfer function P_{ma} in the block diagram in Fig. 5

$$P_{\mathrm{VCM}}(s) = P_{\mathrm{ma}}(s)P_E(s), \quad P_{\mathrm{MA}}(s) = P_{\mathrm{ma}}(s)P_D(s) \tag{42}$$

Here, the E-block P_E and suspension P_{ma} dynamics are assumed to have structures as

$$P_E(s) = P_F(s)P_B(s) \tag{43}$$

$$P_{\mathrm{ma}}(s) = P_{T1}(s)P_S(s)P_{T2}(s) \tag{44}$$

where each term of the right-hand sides is of the form

$$P_j(s) = \frac{b_0^j s^2 + b_1^j s + b_2^j}{s^2 + a_1^j s + a_2^j}, \quad j = F,B,T1,S,T2 \tag{45}$$

with uncertain coefficients

$$b_k^j = \bar{b}_k^j(1 + M_{bk}^j \delta^j), \quad k = 1,2 \tag{46}$$

$$a_k^j = \bar{a}_k^j(1 + M_{ak}^j \delta^j), \quad k = 1,2 \tag{47}$$

Here, the nominal values are denoted by $\bar{a}_k^j$ and $\bar{b}_k^j$, and M_{ak}^j and M_{bk}^j are the constant weightings. It has been found that the experimental frequency responses can be reproduced accurately enough by using only three uncertain parameters

$$\delta_1 = \delta^F, \quad \delta_2 = \delta^B, \quad \delta_3 = \delta^{T1} = \delta^{T2} = \delta^S \tag{48}$$

P_D is the piezoelectric actuator driver dynamics that is not observed in P_{VCM}, and of the form

$$P_D(s) = b_1^D s + b_2^D \tag{49}$$

Assuming the structure of the model (42)–(49), the nominal values and the weighting coefficients are identified as in Table 1. The validity of the modeling result will be examined after the discretization of the model set in Sec. 5.2.

5.2 Discretization of a Continuous-Time Model Set. For digital controller design, the continuous-time uncertain model is transformed into a discrete-time one. Although there are several ways to carry out such transformation, we present only one method here.

The block diagram in Fig. 5 can be expressed as a linear fractional transformation (LFT) form with uncertain parameters, as in Fig. 6. We can represent the continuous-time model set from $[u_V, u_M]^T$ to y_{LDV} as

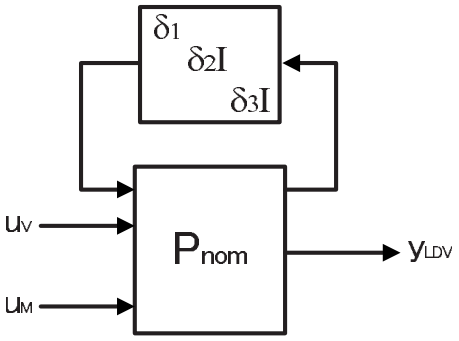

Fig. 6 Block diagram with parametric uncertainties

$$\mathcal{P}_c = \left\{ \begin{matrix} P(s) = D + C(sI - A(\Delta))^{-1}B(\Delta) \\ \Delta = \mathrm{diag}[\delta_1, \delta_2 I, \delta_3 I], \ |\delta_i| \le 1, \forall\, i \end{matrix} \right\} \tag{50}$$

Since there are three uncertain parameters δ_i, the set $\mathcal{P}_c$ has 2^3 "extreme" cases denoted by Δ_i, where each parameter δ_i takes the value of -1 or 1. For each extreme case, we transform the continuous-time model into a discrete-one by zero-order hold, yielding discrete-time (A,B)-matrices as follows:

$$A_d^i := e^{A(\Delta_i)T}, \quad B_d^i := \int_0^T e^{A(\Delta_i)\tau} d\tau B(\Delta_i)$$

where $T = 25 \times 10^{-6}$ (s) is a sampling period. For controller design, we use all the convex combinations of these eight discrete-time (A,B)-matrices:

$$\mathcal{P}_d := \{P(z) = D + C(zI - A)^{-1}B, \ [A,B] \in \mathcal{B}\}$$

where

$$\mathcal{B} := \left\{ [A,B] = \sum_{i=1}^{8} \alpha_k [A_d^i, B_d^i], \ \alpha_i \ge 0, \sum_{i=1}^{8} \alpha_i = 1 \right\}$$

The comparisons between experimental frequency responses and those of sampled models in the model set $\mathcal{P}_d$ are shown in Figs. 7 and 8. Both figures show that the observed dynamic variation can be accurately represented by the parametric uncertainty modeling technique.

5.3 Controller Design via Robust H_2 Synthesis. To determine a controller design problem, we need to specify the variables z_2, w_2, y, and u in Eq. (37). In this example, control inputs u are taken as

$$u := [u_V, u_M]^T$$

As a disturbance, in this simple example, we consider only track runout r, modeled as

$$r = W_r w_2$$

where W_r is a shaping filter

Table 1 Nominal parameters and weighting coefficient values

Mode j	$\bar{b}_0^j$	$\bar{b}_1^j$	$\bar{b}_2^j$	$\bar{a}_1^j$	$\bar{a}_2^j$	M_{b1}^j	M_{b2}^j	M_{a1}^j	M_{a2}^j
F	0	0	4.206×10^8	51.175	2.365×10^4	0	0.3	0	0
B	0	0	1.003×10^9	569.8	1.003×10^9	0	0.35	0	0.35
$T1$	1	720	1.598×10^9	208.2	1.575×10^9	−0.03	−0.03	0	0.05
S	0	0	3.316×10^9	1015	3.316×10^9	0	0.12	0.1	0.12
$T2$	1	6300	1.079×10^{10}	2700	1.02×10^{10}	−0.01	−0.01	0	0.05
D	–	4.0026×10^{-4}	47.3151	–	–				

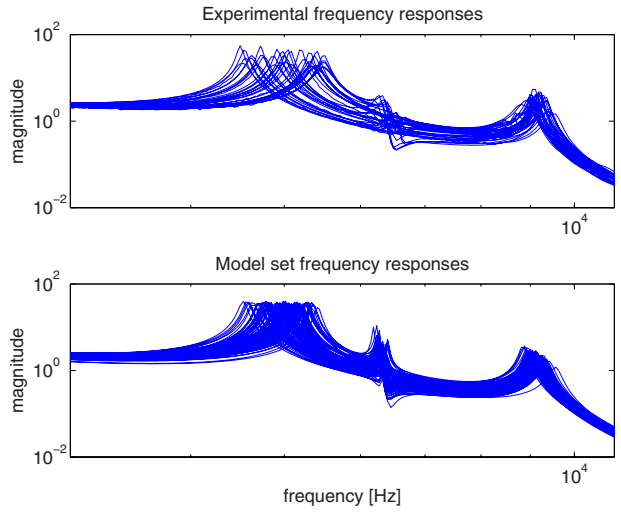

Fig. 7 Comparisons between the experimental and simulation frequency responses for P_{VCM}

$$W_r(s) = \frac{3.162s + 1.987 \times 10^5}{s + 628.3}$$

and w_2 is white noise (this w_2 corresponds to the one in Eq. (37)). The difference between r and y_{LDV}

$$e := r - y_{\mathrm{LDV}}$$

is the PES, which is the measurement y in Eq. (37). As the control outputs z, we use the vector consisting of the PES and weighted input signals as

$$z := [e, Q_V u_V, Q_M u_M]^T$$

where the weights Q_V and Q_M are selected by trial-and-error as $Q_V = 0.1$ and $Q_M = 5 \times 10^{-5}$.

The designed controller was of order 13. In order to analyze the controller, the sensitivity functions for 100 sampled models are shown in Fig. 9. As can be seen in the figure, the sensitivity functions do not disperse even in the face of parameter variations, indicating that the obtained controller indeed satisfies its intended robust performance property. This property was also verified during the experimental tests, as discussed in Ref. [21].

The shaping of the closed-loop sensitivity transfer function can

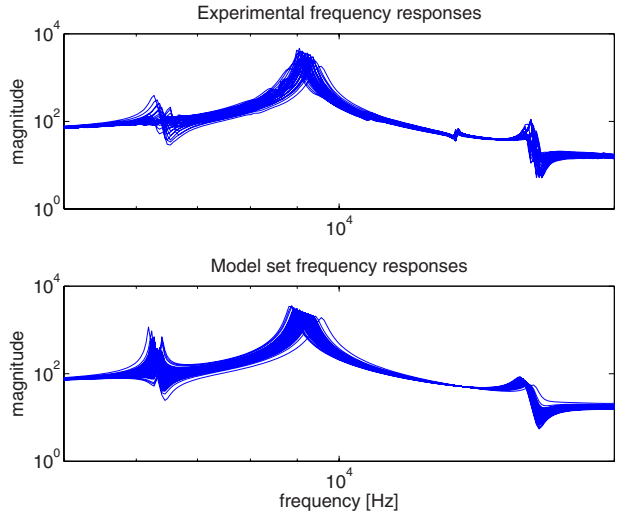

Fig. 8 Comparisons between the experimental and simulation frequency responses for P_{MA}

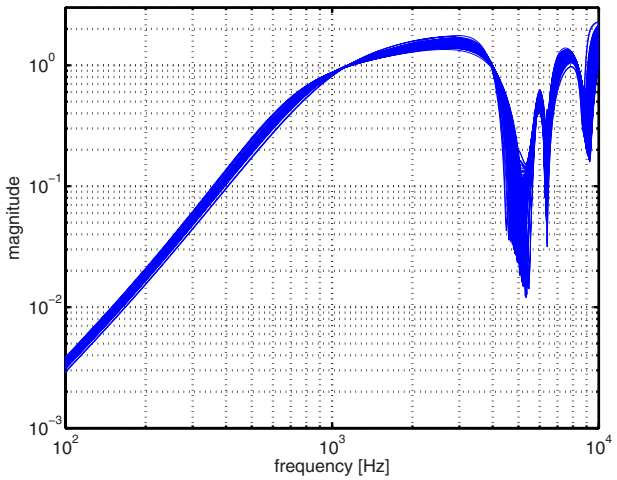

Fig. 9 Sensitivity functions

be achieved by properly selecting the runout model. The selection of the runout model is in fact a design parameter in our synthesis methodologies, and the one selected lead to a reasonable sensitivity function. In general, the magnitude frequency response of the sensitivity function tends to follow the inverse of the magnitude of the runout model, subjected to the constraints imposed by the other weighting terms in the H_2 cost function and the robustness constraints [22]. The systematic and optimal design of a runout model from actual PES data is an important research subject, which is actively carried out by the disk drive companies [24,25].

6 Conclusions

In this paper, we have presented three multirate robust controller design methods for track-following control in dual-stage multisensing servo systems. The procedures, advantages, and disadvantages have been provided for each method. In addition, multirate control problems have been shown to be reduced to time-invariant control problems. All of the methods rely on numerically efficient solvers for LMIs. This paper can be seen as a collection of results from the robust control literature, including those in Refs. [1,2,18,13], which are specially useful for track-following controller design in dual-stage HDDs. One track-following control example for a PZT-actuated suspension dual-stage system was given to illustrate that the robust H_2 controller is useful in maintaining the track-following performance under plant perturbations.

It is known that one major drawback of robust control theory is that the designed controllers typically have high orders. Therefore, controller reduction should also be done after all of the three proposed design procedures. Since a multirate controller is periodic time-varying in general, we can utilize the existing balanced truncation techniques, e.g., those in Refs. [26,27], for the reduction purpose. Some realistic examples in Ref. [3] show that our design methods plus model reduction are quite promising in designing low order controllers with robust track-following performance. Finally, fixed-order controller design such as the one presented in Ref. [20] will be useful in this application, which is a future research topic.

Acknowledgment

The authors are grateful to Professor Raymond de Callafon at the Mechanical Engineering Department of the University of California, San Diego, CA, for providing the experimental data used in the dual-stage servo example presented in this paper. This work was supported by the Information Storage Industry Consortium (INSIC), the Computer Mechanics Laboratory (CML) at UC Berkeley, the Swedish Research Council (VR) and the National Sci-

ence Foundation under Grant No. CMS-0428917.

Appendix A: LMIs for Mixed H_2/H_∞ Synthesis

Here, we present LMIs used for our mixed H_2/H_∞ design in Sec. 4.1. These LMIs can be derived by combining the ideas of congruent transformations in Ref. [11] and of synthesis for time-varying systems in Refs. [1,4]. We use the following notation: For a block-diagonal matrix $\boldsymbol{M}$ and a shift matrix Z (see Eq. (19)) with appropriate block sizes, we define

$$\boldsymbol{M}_Z := Z^T \boldsymbol{M} Z \tag{A1}$$

Note that $\boldsymbol{M}_Z$ is also block-diagonal.

Using the system matrices in Eq. (27) and block diagonal decision variables $\boldsymbol{W}=\boldsymbol{W}^T$, $\boldsymbol{X}=\boldsymbol{X}^T$, $\boldsymbol{Y}=\boldsymbol{Y}^T$, $\hat{\boldsymbol{K}}_A$, $\hat{\boldsymbol{K}}_B$, $\hat{\boldsymbol{K}}_C$, and $\hat{\boldsymbol{K}}_D$ with appropriate sizes, the optimization problem Eq. (26) is equivalent to

$$\min \text{trace}\boldsymbol{W}, \text{subject to} \begin{bmatrix} \boldsymbol{W} & \boldsymbol{C}_2 + \boldsymbol{D}_{2u}\hat{\boldsymbol{K}}_D\boldsymbol{C}_y & \boldsymbol{C}_2\boldsymbol{Y} + \boldsymbol{D}_{2u}\hat{\boldsymbol{K}}_C & \boldsymbol{D}_{22} + \boldsymbol{D}_{2u}\hat{\boldsymbol{K}}_D\boldsymbol{D}_{y2} \\ * & \boldsymbol{X} & I & 0 \\ * & * & \boldsymbol{Y} & 0 \\ * & * & * & I \end{bmatrix} > 0$$

$$\begin{bmatrix} \boldsymbol{X}_Z & I & \boldsymbol{X}_Z\boldsymbol{A} + \hat{\boldsymbol{K}}_B\boldsymbol{C}_y & \hat{\boldsymbol{K}}_A & \boldsymbol{X}_Z\boldsymbol{B}_2 + \hat{\boldsymbol{K}}_B\boldsymbol{D}_{y2} \\ * & \boldsymbol{Y}_Z & \boldsymbol{A} + \boldsymbol{B}_u\hat{\boldsymbol{K}}_D\boldsymbol{C}_y & \boldsymbol{A}\boldsymbol{Y} + \boldsymbol{B}_u\hat{\boldsymbol{K}}_C & \boldsymbol{B}_2 + \boldsymbol{B}_u\hat{\boldsymbol{K}}_D\boldsymbol{D}_{y2} \\ * & * & \boldsymbol{X} & I & 0 \\ * & * & * & \boldsymbol{Y} & 0 \\ * & * & * & * & I \end{bmatrix} > 0$$

$$\begin{bmatrix} \boldsymbol{X}_Z & I & \boldsymbol{X}_Z\boldsymbol{A} + \hat{\boldsymbol{K}}_B\boldsymbol{C}_y & \hat{\boldsymbol{K}}_A & \boldsymbol{X}_Z\boldsymbol{B}_i + \hat{\boldsymbol{K}}_B\boldsymbol{D}_{yi} & 0 \\ * & \boldsymbol{Y}_Z & \boldsymbol{A} + \boldsymbol{B}_u\hat{\boldsymbol{K}}_D\boldsymbol{C}_y & \boldsymbol{A}\boldsymbol{Y} + \boldsymbol{B}_u\hat{\boldsymbol{K}}_C & \boldsymbol{B}_i + \boldsymbol{B}_u\hat{\boldsymbol{K}}_D\boldsymbol{D}_{yi} & 0 \\ * & * & \boldsymbol{X} & I & 0 & \boldsymbol{C}_i^T + \boldsymbol{C}_y^T\hat{\boldsymbol{K}}_D^T\boldsymbol{D}_{iu}^T \\ * & * & * & \boldsymbol{Y} & 0 & \boldsymbol{Y}\boldsymbol{C}_i^T + \hat{\boldsymbol{K}}_C^T\boldsymbol{D}_{iu}^T \\ * & * & * & * & \boldsymbol{D}_{ii}^T + \boldsymbol{D}_{yi}^T\hat{\boldsymbol{K}}_D^T\boldsymbol{D}_{iu}^T & \\ * & * & * & * & * & I \end{bmatrix} > 0 \tag{A2}$$

where $i=V,M$. Note that all the entries in the above LMIs are block-diagonal. For the controller reconstruction, we first compute for block-diagonal nonsingular matrices $\boldsymbol{M}$ and $\boldsymbol{N}$, having the same block structure as $\boldsymbol{X}$ and $\boldsymbol{Y}$, and satisfying

$$\boldsymbol{M}\boldsymbol{N}^T = I - \boldsymbol{X}\boldsymbol{Y} \tag{A3}$$

The controller matrices are given by

$$\boldsymbol{K}_D = \hat{\boldsymbol{K}}_D \tag{A4}$$

$$\boldsymbol{K}_C = (\hat{\boldsymbol{K}}_C - \hat{\boldsymbol{K}}_D\boldsymbol{C}_y\boldsymbol{Y})\boldsymbol{N}^{-T} \tag{A5}$$

$$\boldsymbol{K}_B = \boldsymbol{M}_Z^{-1}(\hat{\boldsymbol{K}}_B - \boldsymbol{X}_Z\boldsymbol{B}_2\hat{\boldsymbol{K}}_D) \tag{A6}$$

$$\boldsymbol{K}_A = \boldsymbol{M}_Z^{-1}\{\hat{\boldsymbol{K}}_A - \boldsymbol{X}_Z(\boldsymbol{A} + \boldsymbol{B}_u\hat{\boldsymbol{K}}_D\boldsymbol{C}_y)\boldsymbol{Y} - \boldsymbol{X}_Z\boldsymbol{B}_u\boldsymbol{K}_C\boldsymbol{N}^T - \boldsymbol{M}_Z\boldsymbol{K}_B\boldsymbol{C}_y\boldsymbol{Y}\}\boldsymbol{N}^{-T} \tag{A7}$$

Note that the block structures of $\boldsymbol{K}_A$, $\boldsymbol{K}_B$, $\boldsymbol{K}_C$, and $\boldsymbol{K}_D$ are guaranteed in the computations, since all the matrices in the right-hand sides of Eqs. (A4)–(A7) are block-diagonal. The corresponding periodic time-varying controller can be obtained by dividing these block matrices, as in Eq. (22).

Appendix B: Initial Controller Design in Robust H_2 Synthesis

As has been explained, the robust H_2 controller is designed via nonconvex optimization (41). For nonconvex optimization, selection of an initial point is of great importance. Here, we review a reasonable method for such selection proposed in Ref. [18].

B.1 State Feedback. First, for the uncertain system (39), we design a state feedback controller as

$$\boldsymbol{u} = \boldsymbol{K}_c\boldsymbol{x} \tag{B1}$$

that optimizes robust H_2 performance

$$\max_{\Delta \in \mathcal{B}_p} \|T_{z_2 w_2}\|_2 \tag{B2}$$

As given in theorem 6 in Ref. [18], this problem can be solved by convex optimization with LMIs:

$$\min_{\boldsymbol{W},\boldsymbol{Q},\boldsymbol{L}} \text{trace}\boldsymbol{W}, \text{ subject to} \begin{cases} \begin{bmatrix} \boldsymbol{W} & \boldsymbol{C}_2^\Delta\boldsymbol{Q} + \boldsymbol{D}_{2u}^\Delta\boldsymbol{L} & \boldsymbol{D}_{22}^\Delta \\ * & \boldsymbol{Q} & 0 \\ * & * & I \end{bmatrix} > 0 \\ \begin{bmatrix} \boldsymbol{Q}_Z & \boldsymbol{A}^\Delta\boldsymbol{Q} + \boldsymbol{B}_u^\Delta\boldsymbol{L} & \boldsymbol{B}_2^\Delta \\ * & \boldsymbol{Q} & 0 \\ * & * & I \end{bmatrix} > 0 \end{cases} \tag{B3}$$

where the constraints are imposed at the vertices of $\mathcal{B}_p$, $\Delta=\Delta_k \in \mathcal{V}(\mathcal{B}_p)$. Using the solutions $\boldsymbol{L}$ and $\boldsymbol{Q}$, the optimal state feedback is given by

$$\boldsymbol{K}_C := \boldsymbol{L}\boldsymbol{Q}^{-1} \tag{B4}$$

B.2 Output Feedback. Next, by fixing $\boldsymbol{K}_C$ in Eq. (B4) and $\boldsymbol{K}_D=0$, we design an output feedback

$$\boldsymbol{u} = \left[\begin{array}{c|c} \boldsymbol{Z}\boldsymbol{K}_A & \boldsymbol{Z}\boldsymbol{K}_B \\ \hline \boldsymbol{K}_C & 0 \end{array}\right]\boldsymbol{y} \tag{B5}$$

that optimizes robust H_2 performance (B2). Define

$$\boldsymbol{A}_F^{\Delta} := \boldsymbol{A}^{\Delta} + \boldsymbol{B}_u^{\Delta}\boldsymbol{K}_C \tag{B6}$$

Then, due to Theorem 8 in Ref. [18], this problem can be solved by convex optimization with LMIs:

$$\min_{\boldsymbol{W},\boldsymbol{X},\boldsymbol{Y},\boldsymbol{U},\boldsymbol{V}} \text{trace}\boldsymbol{W}, \text{ subject to} \begin{cases} \begin{bmatrix} \boldsymbol{W} & \boldsymbol{C}_z^{\Delta} + \boldsymbol{D}_{zu}^{\Delta}\boldsymbol{K}_C & \boldsymbol{D}_{zu}^{\Delta}\boldsymbol{K}_C & \boldsymbol{D}_{zw}^{\Delta} \\ * & \boldsymbol{X} & 0 & 0 \\ * & * & \boldsymbol{Y} & 0 \\ * & * & * & \boldsymbol{I} \end{bmatrix} > 0 \\ \begin{bmatrix} \boldsymbol{X}_Z & 0 & \boldsymbol{X}_Z\boldsymbol{A}_F^{\Delta} & -\boldsymbol{X}_Z\boldsymbol{B}_u^{\Delta}\boldsymbol{K}_C & \boldsymbol{X}_Z\boldsymbol{B}_w^{\Delta} \\ * & \boldsymbol{Y}_Z & \boldsymbol{Y}_Z\boldsymbol{A}_F^{\Delta} - \boldsymbol{V} - \boldsymbol{U}\boldsymbol{C}_y & \boldsymbol{V} - \boldsymbol{Y}_Z\boldsymbol{B}_u^{\Delta}\boldsymbol{K}_C & \boldsymbol{Y}_Z\boldsymbol{B}_w^{\Delta} - \boldsymbol{U}\boldsymbol{D}_{yw} \\ * & * & \boldsymbol{X} & 0 & 0 \\ * & * & * & \boldsymbol{Y} & 0 \\ * & * & * & * & \boldsymbol{I} \end{bmatrix} \end{cases} \tag{B7}$$

where the constraints are again imposed at the vertices of $\mathcal{B}_p$, $\Delta = \Delta_k \in \mathcal{V}(\mathcal{B}_p)$. Using the optimizers, $\boldsymbol{K}_A$ and $\boldsymbol{K}_B$ are obtained as

$$\boldsymbol{K}_A := \boldsymbol{Y}_Z^{-1}\boldsymbol{V}, \quad \boldsymbol{K}_B := \boldsymbol{Y}_Z^{-1}\boldsymbol{U} \tag{B8}$$

References

[1] Dullerud, G. E., and Lall, S., 1999, "A New Approach for Analysis and Synthesis of Time-Varying Systems," IEEE Trans. Autom. Control, **44**(8), pp. 1486–1497.

[2] Lall, S., and Dullerud, G., 2001, "An LMI Solution to the Robust Synthesis Problem for Multi-Rate Sampled-Data Systems," Automatica, **37**(12), pp. 1909–1922.

[3] Huang, X., Nagamune, R., and Horowitz, R., 2006, "A Comparison of Multirate Robust Track-Following Control Synthesis Techniques for Dual-Stage and Multisensing Servo Systems in Hard Disk Drives," IEEE Trans. Magn., **42**(7), pp. 1896–904.

[4] Peters, M. A., and Iglesias, P. A., 1997, *Minimum Entropy Control for Time-Varying Systems. Systems & Control: Foundations & Applications*, Birkhäuser, Boston, MA.

[5] Nesterov, Y., and Nemirovskii, A., 1994, *Interior-Point polynomial Algorithms in Convex Programming*, SIAM, Philadelphia, PA.

[6] Sturm, J. F., 1999, "Using SEDUMI 1.02, a MATLAB Toolbox for Optimization Over Symmetric Cones," (Special Issue on Interior Point Methods), Optim. Methods Software, **11**, pp. 625–653.

[7] Gahinet, P., Nemirovski, A., Laub, A. J., and Chilali, M., 1995, *LMI Control Toolbox User's Guide*, The MathWorks, Inc., Natick, MA.

[8] Löfberg, J., 2004, "YALMIP: A Toolbox for Modeling and Optimization in MATLAB," *Proceedings of the CACSD Conference*, Taipei, Taiwan. Available from http://control.ee.ethz.ch/~joloef/yalmip.php

[9] Bernstein, D. S., and Haddad, W. H., 1989, "LQG Control With an H_∞ Performance Bound: A Riccati Equation Approach," IEEE Trans. Autom. Control, **34**(3), pp. 293–305.

[10] Khargonekar, P., and Rotea, M., 1991, "Mixed H_2/H_∞ Control: A Convex Optimization Approach," IEEE Trans. Autom. Control, **36**, pp. 824–837.

[11] Scherer, C., Gahinet, P., and Chilali, M., 1997, "Multiobjective Output-Feedback Control via LMI Optimization," IEEE Trans. Autom. Control, **42**(7), pp. 896–911.

[12] Masubuchi, I., Ohara, A., and Suda, N., 1998, "LMI-Based Controller Synthesis: A Unified Formulation and Solution," Int. J. Robust Nonlinear Control, **8**(8), pp. 669–686.

[13] Packard, A., and Doyle, J. C., 1993, "The Complex Structured Singular Value," Automatica, **29**(1), pp. 71–109.

[14] Young, P. M., 1996, "Controller Design With Real Parametric Uncertainty," Int. J. Control, **65**(3), pp. 469–509.

[15] Balas, G., Chiang, R., Packard, A., and Safonov, M., 2005, *Robust Control Toolbox for Use With MATLAB*, The Mathworks, Inc., Natick, MA.

[16] Young, P. M., and Doyle, J. C., 1996, "Properties of the Mixed μ Problem and Its Bounds," IEEE Trans. Autom. Control, **41**(1), pp. 155–159.

[17] Tits, A. L., and Chou, Y. S., 2000, "On Mixed-μ Synthesis," Automatica, **36**, pp. 1077–1079.

[18] Kanev, S., Scherer, C., Verhaegen, M., and De Schutter, B., 2004, "Robust Output-Feedback Controller Design via Local BMI Optimization," Automatica, **40**, pp. 1115-1127.

[19] Iwasaki, T., and Skelton, R. E., 1995, "The XY-Centering Algorithm for the Dual LMI Problem: A New Approach to Fixed Order Control Design," Int. J. Control, **62**(6), pp. 1257–1272.

[20] Iwasaki, T., 1999, "The Dual Iteration for Fixed-Order Control," IEEE Trans. Autom. Control, **44**(4), pp. 783–788.

[21] de Callafon, R. A., Nagamune, R., and Horowitz, R., 2006, "Robust Dynamic Modeling and Control of Dual-Stage Actuators," IEEE Trans. Magn., **42**(2), pp. 247–54.

[22] Li, Y., and Horowitz, R., 2002, "Design and Testing of Track-Following Controllers for Dual-Stage Servo Systems With PZT Actuated Suspensions," Microsyst. Technol., **8**, pp. 194–205.

[23] Li, Y., Marcassa, F., Horowitz, R., Oboe, R., and Evans, R., 2003, "Track-Following Control With Active Vibration Damping of a PZT-Actuated Suspension Dual-Stage Servo System," *Proceedings of the American Control Conference*, Vol. 3.

[24] Abramovitch, D., Hurst, T., and Henze, D., 1998, "An Overview of the PES Pareto Method for Decomposing Baseline Noise Sources in Hard Disk Position Error Signals," IEEE Trans. Magn., **34**(1), pp. 17–23.

[25] Ehrlich, R., and Curran, D., 1999, "Major HDD TMR Sources and Projected Scaling With TPI," IEEE Trans. Magn., **35**, pp. 885–891.

[26] Varga, A., 2000, "Balanced Truncation Model Reduction of Periodic Systems," *Proceedings of the 39th IEEE Conference on Decision and Control*, Sydney, Australia, pp. 2379–2384.

[27] Sandberg, H., and Rantzer, A., 2004, "Balanced Truncation of Linear Time-Varying Systems," IEEE Trans. Autom. Control, **49**(2), pp. 217–229.